International Journal of Astrophysics and Space Science
2021; 10(2): 18-27
http://www.sciencepublishinggroup.com/j/ijass
doi: 10.11648/j.ijass.20221002.11
ISSN: 2376-7014 (Print); ISSN: 2376-7022 (Online)

Effects of Geomagnetic Storm on Ionospheric TEC Variability over High Latitude Regions

Chali Idosa Uga

Department of Physics, Faculty of Natural Science, Jimma University, Jimma, Ethiopia

Email address:
chaleidosa2011@gmail.com, chali.edosa@ju.edu.et

To cite this article:
Chali Idosa. Effects of Geomagnetic Storm on Ionospheric TEC Variability over High Latitude Regions. *International Journal of Astrophysics and Space Science*. Vol. 10, No. 2, 2022, pp. 18-27. doi: 10.11648/j.ijass.20221002.11

Received: June 24, 2022; **Accepted:** July 26, 2022; **Published:** August 10, 2022

Abstract: The effects of the geomagnetic storm on August 26, 2018 on the ionospheric TEC fluctuations in the high latitude region were investigated. This study is based on TEC data obtained by the UNAVCO dual-frequency GPS devices at the northern stations of Hofn and Kiruna, and the southern stations of Mawson and Syog. The results of this study show that the variation of TEC is more noticeable in the northern hemisphere of the Hofn and Kiruna stations than in the southern hemisphere of the Mawson and Syog stations on the August 26, 2018 storm. Interestingly, the midnight TEC became comparable to the daytime TEC over both northern and southern stations, indicating the ingestion of additional plasma from higher latitudes into the northern stations. The positive enhancement of ΔTEC values were higher over Hofn and Kiruna on August 26, 2018 by about 170%, and 180% than Mawson and Syog by about 70%, and 150% stations, respectively. During geomagnetic storm of August 26, 2018, the Hofn and Kiruna stations had a much greater negative impact on ΔTEC = -50% than the Mawson and Syog stations ΔTEC = -40%. The ΔTEC over each station are caused by a significant rise in the Kp index and the opposite polarity of the interplanetary electric field (IEF Ey) in the northward direction and the southward decrease of the interplanetary magnetic field (IMF Bz). The decrease in Dst-index and ΔH during the main phase of the storm increased TEC over Kiruna and Mawson stations. Furthermore, the values of changes in TEC was stronger over Kiruna station in the northern hemisphere than over Mawson station in the southern hemisphere, indicating that the northern stations received more additional plasma than the southern stations during the August 26, 2018 geomagnetic storm. During the August 26, 2018 geomagnetic storm, the values of the horizontal component of Earth's magnetic field decreased more over Kiruna station, about ΔH = -1500 nT, than over Mawson station, about ΔH = -1300 nT. As a result, the changes in TEC are more pronounced over Kiruna station, where ΔTEC = 180%, than over Mawson station, where ΔTEC = 70%. This indicates that during the August 26, 2018 geomagnetic storm, the northern hemisphere receives more energy from the solar wind, which produces particle acceleration and precipitation, higher field aligned currents, and ionospheric electrojets.

Keywords: Ionospheric TEC, Geomagnetic Storm, TEC Enhancement, TEC Variability

1. Introduction

The effective movement of energy from solar wind eruptions from the sun's active regions into the Earth's magnetosphere causes massive disruptions known as geomagnetic storms [1]. Such disruptions create perturbations in the charged particles of the ionosphere, which can have a negative impact on radio-wave transmissions and satellite communications. These effects have been claimed to be particularly pronounced in the earth's ionosphere's equatorial regions, where considerable changes in ionospheric parameters have been seen, owing to the presence of a ring current moving in the equatorial plane [2, 3, 4].

When high-speed plasma released into the solar wind by coronal mass ejections or coronal holes interacts with Earth's geomagnetic field, geomagnetic storms occur [5]. If the incoming solar wind plasma has a southward magnetic field, energy is efficiently transmitted into the magnetosphere and upper atmosphere of Earth [6]. The strength of the low-latitude magnetic index, Dst, which is a measure of the magnetospheric ring current, has come to characterize the scale of the

geomagnetic storm [7, 8]. Although the ring current is not a major determinant of the upper atmosphere, its sources are linked; Dst may reflect the amount of magnetospheric energy input to the upper atmosphere [9, 10].

So, from the perspective of the upper atmosphere, a geomagnetic storm is a period when there is a significant rise in this magnetospheric source for several hours to days [11]. When a storm happens, auroral particle precipitation develops and spreads to lower latitudes than usual, and the magnetospheric electric field mapped to the atmosphere accelerates and spreads in conjunction with the auroral oval [12].

The auroral particles heat and ionize the gas, increasing atmospheric conductivity, and the electric field interacts with the enhanced conductivity to increase Joule heating, the dominant atmospheric energy source during a storm [13].

Under disturbed conditions generated by solar wind magnetosphere coupling, the ionosphere in the auroral regions may become very turbulent, increasing the probability of irregularities forming; these irregularities, on a different scale, create changes in the total electron content (TEC fluctuations) [14, 15].

One of the main topics in space weather effects is the response of the ionospheric TEC to a geomagnetic storm. There are initial, main, and recovery phases of geomagnetic storms following a sudden storm commencement (SSC). The magnetospheric electric field and particle precipitation patterns grow during the initial phase; the electric fields become stronger, and the precipitation intensifies. The Joule and particle heating rates, as well as the electrojet currents, increased during this period. During the main phase, the energy input to the upper atmosphere is greatest, whereas during the recovery phase, geomagnetic activity and energy input are lowest [16].

Large storms may dramatically change the density, composition, and circulation of the ionosphere-thermosphere system on a global scale, and the changes can last for many days after the geomagnetic activity ends. A positive ionospheric storm occurs when electron density increases as a result of storm dynamics, whereas a negative ionospheric storm occurs when electron density decreases [17].

The positive ionospheric storm is explained by increases in oxygen density, changes in meridional winds that lead the ionosphere to higher altitudes with lower recombination rates, an eastward electric field that uplifts the ionosphere while also leading it to lower recombination rates, downward protonospheric plasma fluxes, traveling ionospheric disturbances (TIDs), and plasma redistribution due to disturbed electric fields. The main phase of the storm, on the other hand, is accompanied by changes in neutral composition, which results in a decrease in the O/N2 density ratio attributable to atmospheric disturbances [16, 18].

Many researchers have investigated the variations of the ionospheric total electron concentration (TEC) over different regions of the ionosphere as [19, 20, 21, 22, 23, 24, 25] and [26]. Large-scale fluctuations are produced by ionospheric irregularities larger than 100-350 km in scale and manifest as significant spatial changes in TEC [27]. With different satellite signals, the formation of TEC variations over high latitude regions of the Earth has been examined [28].

To study the impacts of geomagnetic storms on the ionospheric TEC variations, Global Positioning System (GPS) observations can provide us with measurements from which TEC can be estimated [29, 30].

The author presents and discusses the ionospheric TEC variability in high latitude sectors as a result of the intense geomagnetic storm of solar cycle 24 that occurred on August 26, 2018, with the minimum Dst index reaching -180 nT at 08:00 UT in this paper. To describe variation and explain the ionosphere's dynamical condition, the ionospheric TEC is highly helpful.

The coupling of the magnetosphere and solar wind causes the ionospheric TEC to respond to the geomagnetic field and electric fields imposed by dynamos operating in the Earth's atmosphere [2].

In the present study, the effects of the August 26, 2018 geomagnetic storm on TEC variability over the high latitude regions of northern and southern stations are studied. This study is important in understanding the variability of ionospheric TEC over northern and southern stations in high latitude regions due to the effects of the August 26, 2018 geomagnetic storm.

2. Data and Methodology

The TEC values were calculated using data collected by GPS receivers over the high latitude regions of Kiruna and Hofn stations in the northern hemisphere and Mawson and Syog-East Ongle Antarctica stations in the southern hemisphere.

During the August 26, 2018 geomagnetic storm, ionospheric TEC data from four stations were analyzed to investigate ionospheric TEC variability over high latitude stations. The data was obtained using dual-frequency GPS devices from UNAVCO (University NAVSTAR Consortium) (http://www.unavco.org/data/gps-gnssdata/).

The values of the solar wind parameters, such as the interplanetary magnetic field (IMF Bz), interplanetary electric field (IEF Ey), plasma speed (v_x), as well as the Kp and Dst-indices, were taken from the omni data sets website, which can be accessed at the (https://omniweb.gsfc.nasa.gov). The station code with their name, geographical and geomagnetic latitudes and longitudes with the universal time relations with the local time of each station are given in Table 1.

The observational data from four GPS stations: Hofn, Kiruna, Mawson, and Syog stations, was used to find the change in TEC during the geomagnetic storm of August 26, 2018 using Equation 1.

$$dTEC = TECobs - TECq \tag{1}$$

Where TEC_{obs} is TEC during storm days, TEC_q is TEC

during mean quiet days. Changes in TEC in percent over all stations is obtained using Equation 2.

$$\Delta TEC = \frac{TEC_{obs} - TEC_q}{TEC_q} \times 100\% \quad (2)$$

In this study, the magnetometer data assessed from the International Real-Time Magnetic Observatory Network (www.intermagnet.org). It generates one-minute values for the Earth's magnetic field's northward (X), eastward (Y), and vertical (Z) components, while the horizontal component (H) is calculated using Equation 3.

$$H = \sqrt{X^2 + Y^2} \quad (3)$$

The night-time baseline values in the H component Equation 4 were obtained for each day and subtracted from the corresponding magnetometer data sets to obtain the hourly departure of H as expressed by Equation 5 in order to avoid different offset values of various magnetometers. The average of the night-time (23:00-02:00 LT) value of the H component of the Earth's magnetic field was used to calculate the baseline value.

$$H_o = \frac{(H_{23} + H_{24} + H_{01} + H_{02})}{4} \quad (4)$$

Where H_{23} + H_{24} + H_{01} + H_{02} are the hourly values of H at 23:00, 24:00, 01:00 and 02:00 in local time (LT) respectively.

$$H = H(t) - H_o \quad (5)$$

Where t is the time in hours ranging from 01:00 LT to 24:00 LT.

Table 1. *Geographical locations of all stations over high latitude regions.*

Station Code	Station Name	Geogra. Lati.	Geogra. Long	Geomag. Lati.	Geomag. Long	UT
Hofn	Iceland	64.26729^{o}N	344.80208^{o}E	64.533641^{o}N	75.006904 ^{o}E	UT+23:00
Kiro	Kiruna	67.87757^{o}N	21.06023^{o}E	64.312603^{o}N	105.151356^{o}E	UT+1.00
Maw1	Mawson	67.60477^{o}S	62.87072^{o}E	70.136534^{o}S	89.921448^{o}E	UT+4.00
Syog	Syog Ongel	69.00696^{o}S	39.58374^{o}E	66.063887^{o}S	71.441184^{o}E	UT+3.00

3. Results and Discussions

Results based on TEC measurements from four GPS sites such as Kiruna and Hofn in the northern hemisphere; Mawson; and Syog in the southern hemisphere are presented in this section. The findings of this study describe the diurnal variability of TEC, changes in TEC, and solar wind parameters with the changes in TEC during the geomagnetic storm on August 26, 2018 using ionospheric parameters and finally compare the change in value with the horizontal component of the magnetic field and Dst-index over Kiruna in the northern hemisphere and Mawson in the southern hemisphere.

3.1. Diurnal Variations of TEC During the Geomagnetic Storm of August 26, 2018

The most significant sources of ionization and fluctuations in ionospheric TEC are the Sun and its activities [31, 32]. As a result, the ionospheric structure and total electron content change significantly in response to solar-related ionospheric and geomagnetic disturbances [33]. Figure 1 depicts the diurnal fluctuation of ionospheric TEC measured over four GPS stations in high latitude regions during the geomagnetic storm of August 26, 2018. The variations of TEC throughout the northern and southern hemispheres of all stations during the geomagnetic storm's initial (25-08-2018), main (26-08-2018), and recovery (27-08-2018) phases are described below.

On August 25, 2018, the TEC value at the Hofn station reached a maximum of 12.25 TECU around 18:00 UT at midnight. On August 26, 2018, TEC had 7.9 TECU at a day side time of around 04:00 UT over Hofn station. On August 27, 2018, the value of TEC was about 8.6 TECU at night time, between 14:00 UT and 16:00 UT, was observed. At Kiruna station on August 25, 2018, the TEC observed was about 7 TECU at noon, around 09:00 UT (10:00 LT), and about 8 TECU at 17:00 UT (18:00 LT). Also, on August 26, 2018, about 9 TECU of TEC in the morning around 03:00 UT (04:00 LT) was recorded. Finally, on August 27, 2018, the TEC value was about 6.6 TECU at noon time, around 09:00 UT (10:00 LT), and at night time, around 18:00 UT (19:00 LT), over Kiruna station.

Over the Mawson station, the variability of TEC has an average of about 8 TECU around the noon time at 09:00 UT (13:00 LT) and around the midnight time at 19:00 UT (23:00 LT) during the initial phase on August 25, 2018. During the main phase of the storm on August 26, 2018, the value of TEC was about 7.5 TECU at the day side time of around 05:00 UT (09:00 LT). TEC has a value of about 7.4 TECU at noon time, around 06:10 UT (09:10 LT) over Mawson station, despite being in the recovery phase on August 27, 2018 storm. At Syog East-Ongle, TEC has a value of about 7.8 TECU at day side time around 11:30 UT (14:30 LT) during the initial phase of the storm. Although on August 26, 2018, it is raised to a value of about 10 TECU at the day side time of around 04:00 UT (07:00 LT). While during the recovery phase, TEC reaches a value of about 5.8 TECU at noon, around 07:00 UT (10:00 LT).

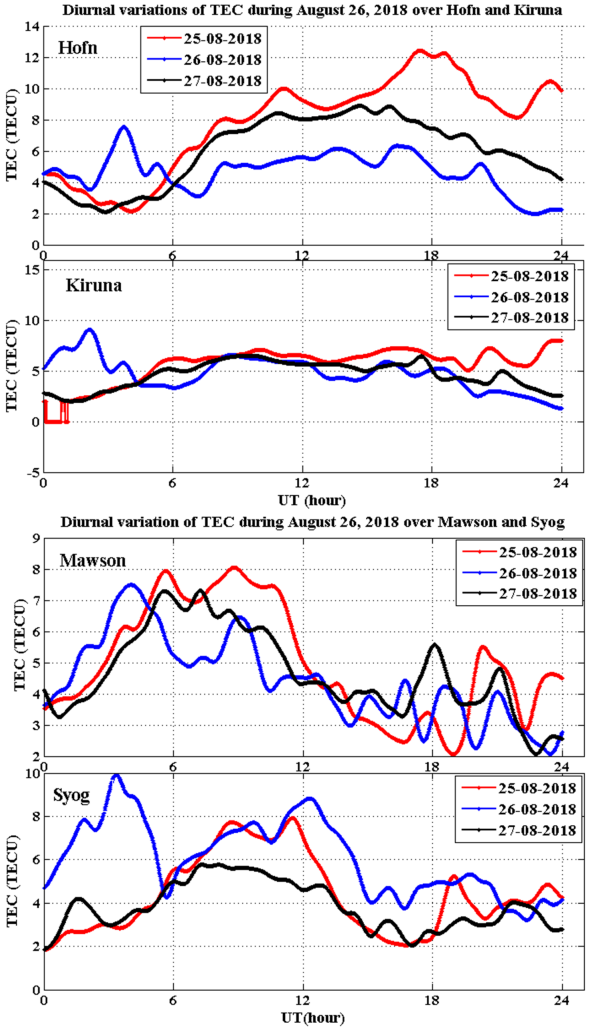

Figure 1. Diurnal variations of TEC over Hofn, Kiruna, Mawson, and Syog stations during the geomagnetic storm of August 25-27/08/2018.

3.2. Variations of TEC During the Geomagnetic Storm of August 26, 2018

The values of ionospheric TEC change with the degree of ionisation, which is typically higher during the day and lower at night [34]. Figure 2 is used to describe the variations of ionospheric TEC over Hofn and Kiruna stations in the northern hemisphere and Mawson and Syog sites in the southern hemisphere of the high latitude area during the geomagnetic storm of August 26, 2018.

TEC increased significantly during the storm's main phase rather than the initial and recovery phases, especially during the daytime. This may be due to the fact that during the dayside time of main phase solar wind-magnetosphere interactions and southward IMF Bz leads to the enhancement of ring current and hermospheric circulation generated by the auroral zone heating during main phase storm time, which in turn influences the enhancement of ionospheric TEC over each sector [35].

In the Kiruna sector, the maximum TEC value was observed during the main phase of the storm at the dayside time of around 02:00 UT (03:00 LT). But over Hofn station, the maximum TEC value was observed during the initial phase of the storm at 18:30 UT (17:30 LT) and during the morning time of the main phase around 03:00 UT. Over the Mawson sector, the maximum TEC value was observed during the initial phase of the storm at around 09:00 UT (13:00 LT) and during the morning time of the main phase at around 04:00 UT. While over Syog station, the maximum TEC value was observed during the main phase of the storm at the day side time of around 02:00 UT to 04:00 UT.

In general, over both the northern and southern hemispheres, the enhancement and variability of ionospheric TEC are observed at different universal times. This is due to the effects of differences in local background solar activity over each sector, i.e., continued sunlit activity in one sector and low sunlit activity in the other, which results in different solar disturbances produced by the sun [31].

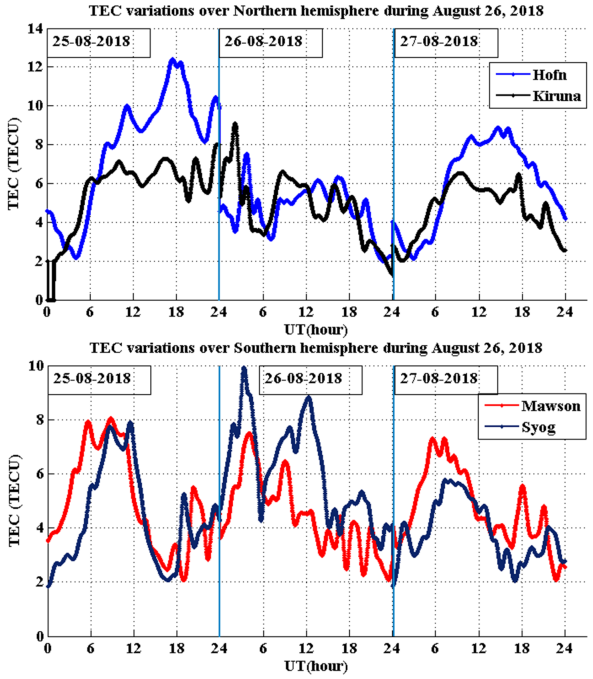

Figure 2. Variability of TEC over two northern and two souther stations during the geomagnetic storm of August 26, 2018.

3.3. Changes in TEC Variability During the Geomagnetic Storm of August 26, 2018

The variability of ionospheric TEC during the geomagnetic storm and during the mean quietest days are explained to understand the positive ionospheric storm and negative ionospheric storm effects over all stations.

Figure 3 shows the values of the changes in TEC (ΔTEC) observed over Hofn, Kiruna, Mawson, and Syog stations.

At Hofn station, during the initial phase of the disturbed time from 06:00 UT (05:00 LT) to 23:59 UT (22:59 LT), a greater value of TEC was observed than on the quiet days. In turn, during the main phase of the observed time, from 00:00 UT to 06:00 UT (05:00 LT), a greater value of TEC was also observed. This TEC variability results in a positive ionospheric ΔTEC value of about 1.9 TEC units and 180% of TEC over Hofn station at around 04:00 UT (03:00 LT). But from about

06:00 UT to 23:59 UT of the main phase, a greater value of TEC was observed during the quiet days than on the observed days. This may lead to a negative ionospheric ΔTEC value of about -1.6 TEC units and -60% of TEC over the Hofn station.

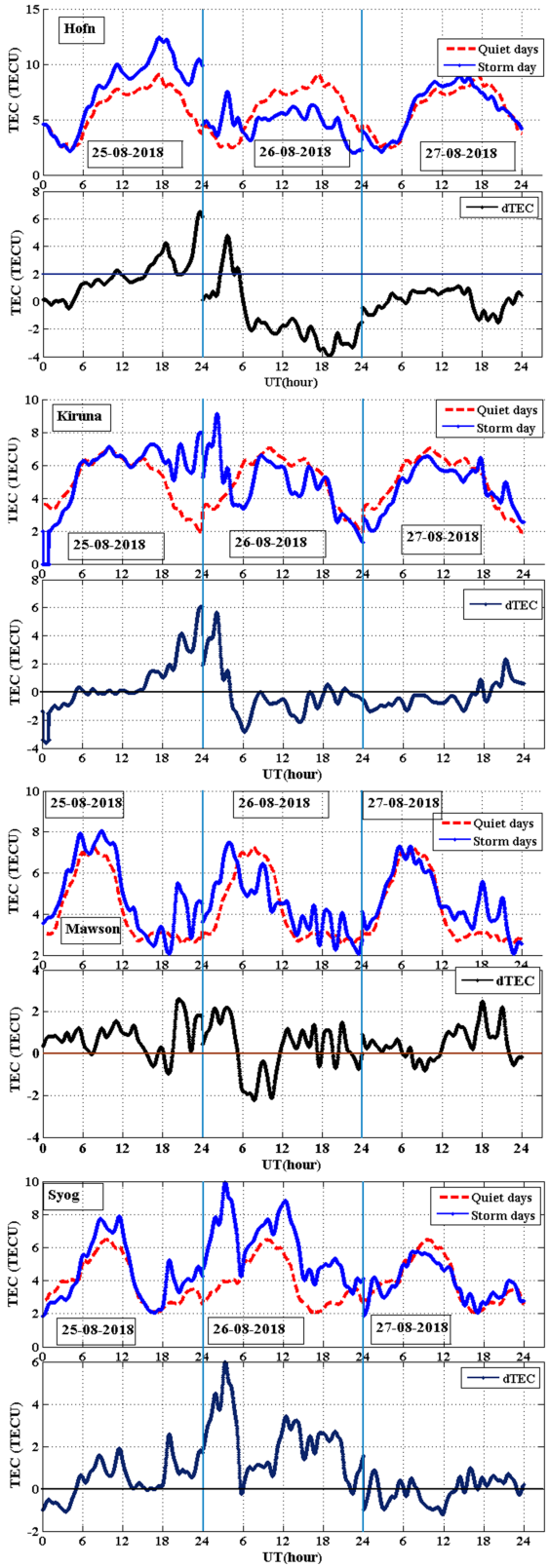

Figure 3. *Change in TEC variations during the geomagnetic storm of August 26, 2018.*

At Kiruna station, during the initial phase of the observed time from 15:00 UT to 23:59 UT, a greater value of TEC was observed than on the quiet days. In turn, during the main phase of the observed time, from 00:00 UT to 05:00 UT, a greater value of TEC was also observed. This TEC variability results in a positive ionospheric ΔTEC value of about 1.8 TEC units and 150% of TEC over Kiruna station at 03:00 UT. But from about 05:00 UT of the main phase to 18:00 UT of the recovery phase, a greater value of TEC was observed during the quiet days than the observed days. This may lead to the negative ionospheric ΔTEC value of about -0.4 TEC units and -50% of TEC over Kiruna station.

At Mawson station, during the initial phase of the observed time from 07:00 UT to 16:00 UT, a greater value of TEC was observed than on the quiet days. Also, from 19:00 UT to 05:30 UT, the main phase of the observed time, a greater value of TEC was also observed. Because of this TEC variability, the initial phase over Mawson station has a positive ionospheric ΔTEC value of about 1 TEC unit and 100% of TEC at around 20:00 UT. But from about 06:00 UT to 12:00 UT of the main phase, a greater value of TEC was observed during the quiet days than on the observed days. This may lead to the negative ionospheric ΔTEC value of about -0.3 TEC units and -30% of TEC over Mawson station at 06:00 UT of the main phase. However, over Syog station, during the initial phase of the observed time from 06:00 UT of the initial phase to 23:00 UT of the main phase, a greater value of TEC was observed during the storm days than the quiet days. These variability of TEC leads to the positive ionospheric ΔTEC value of about 1.5 TEC units and 150% of TEC at around 04:00 UT of main phase over Syog station. But from about 23:00 UT of main phase to 16:00 UT of recovery phase, greater value of TEC was observed during the quiet days than the observed days. This may lead to the negative ionospheric ΔTEC value of about -0.4 TEC units and -40% of TEC over Syog station at 00:00 UT of the recovery phase.

3.4. The Changes in TEC with Solar wind Parameters During the Geomagnetic Storm of August 26, 2018

Figure 4 depicts the variability in the Bz component of the interplanetary magnetic field (IMF), the Ey component of the interplanetary electric field (IEF), plasma speed (v_x), as well as the Kp and Dst indices, and the change in TEC during the August 26, 2018 geomagnetic storm. The Dst-index, as shown in Figure 4, reached a disruption of around -180 nT on August 26, 2018.

During the storm, the southward decreasing of IMF Bz was observed at around -15.2 nT with Kp $>$ 5 (70) when the solar wind plasma speed and IEF Ey recorded values of 400 km/s and 5.83 mV/m, respectively. The Bz component decrease corresponds to the Dst index value. As the Dst-index dropped, the storm occurred during the local day-side hour of the main phase between 07:00 UT and 08:00 UT. The TEC value was raised over both northern and southern hemisphere stations in combination with a large increase in the Kp index value and a declining more negative value of the IMF Bz [36].

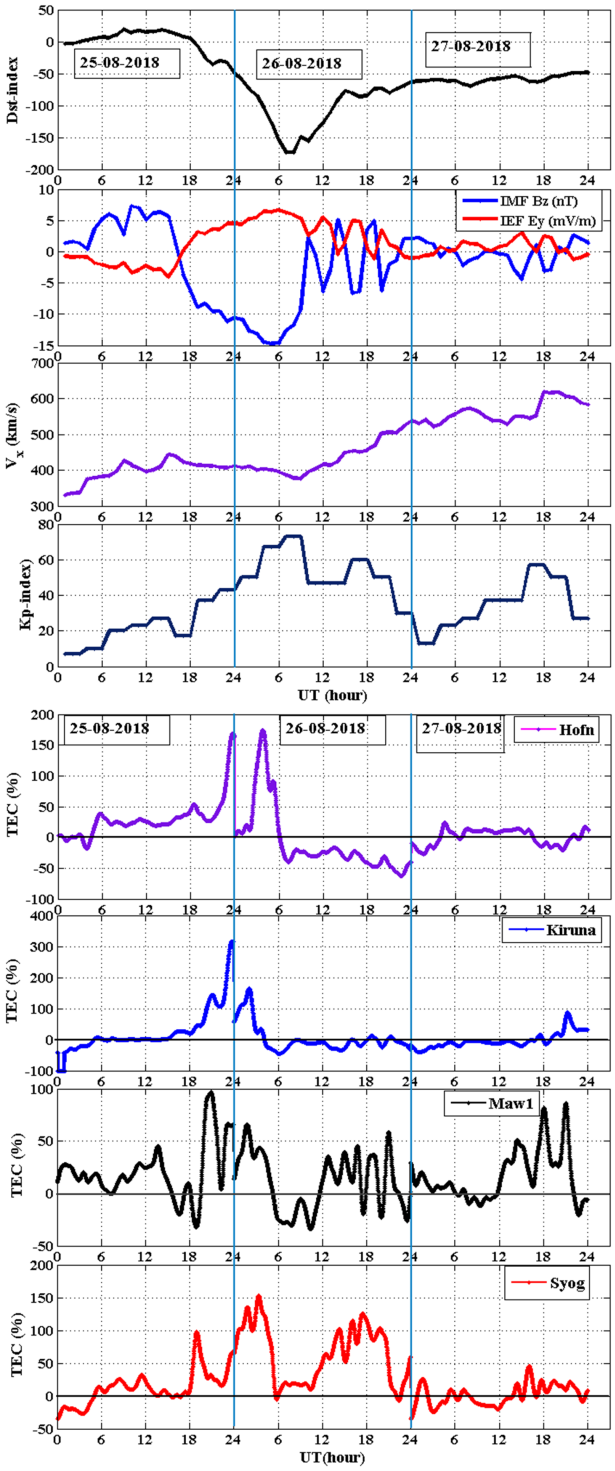

Figure 4. Changes in TEC variations with solar wind parameters over all stations during the geomagnetic storm of August 26, 2018.

3.5. The Variations of Dst Index, Horizontal Magnetic Field and Changes in TEC over Kiruna and Mawson During August 26, 2018

A geomagnetic storm is distinguished by a depression in the H component of the magnetic field induced by ring current owing westward or eastward in the magnetosphere, which may be tracked using the Dst-index [37].

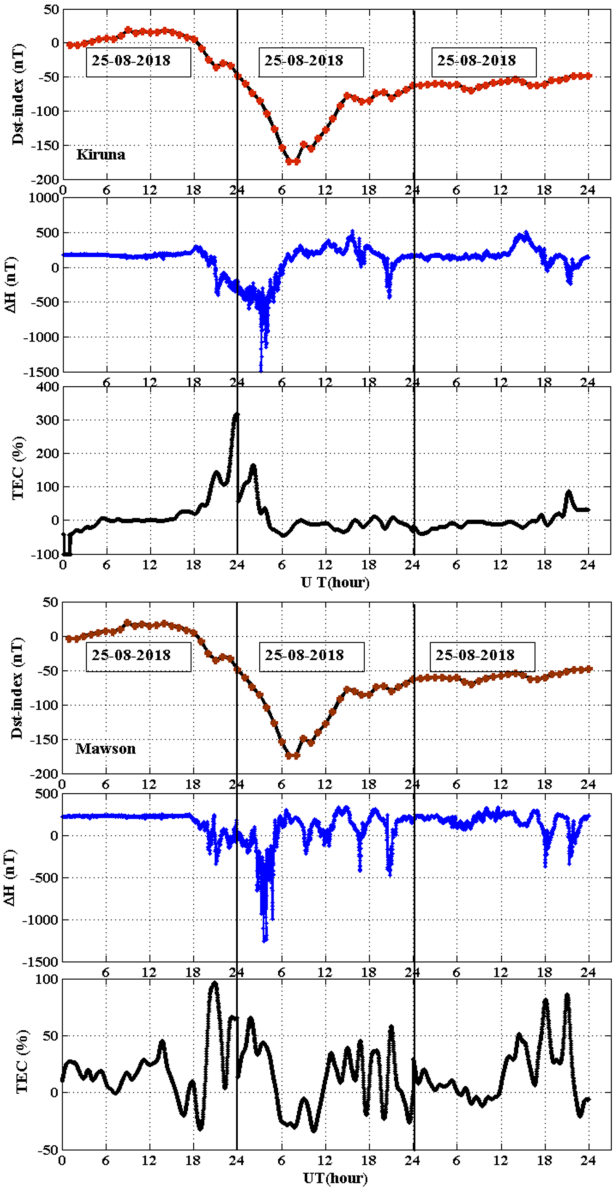

Figure 5. Dst-index, ΔH, and ΔTEC over Kiruna and Mawson stations during the geomagnetic storm of August 26, 2018.

Variations in the horizontal component of the geomagnetic field are caused by interactions between IMF Bz and the magnetosphere. Because of the form and intensity of the Earth's dipole magnetic field, energetic ions travel from midnight to dusk and energetic electrons flow to dawn, according to [6]. The difference in flow directions of positively and negatively charged ions produces an electric current, a ring current that encircles the earth. This ring current, in turn, gives the magnetic field the points opposite the dipole field at the earth's surface. As a result, the ring current weakens the earth's magnetic field as measured on the surface [38].

Figure 5 shows the variability of Dst-index and the horizontal component of the earth's magnetic field (ΔH) with ΔTEC over Kiruna station in the northern hemisphere and Mawson station in the southern hemisphere. One can understand that the decrement of the Dst-index and the

enhancement of the westward aurora lead to a decrease in the horizontal geomagnetic field of the earth of about ΔH =-1500 nT during the day side time around 04:00 UT. With this ΔH decreasing, the ΔTEC value over Kiruna reaches a positive value of around 160%.

At the same time, with the decrement of the Dst-index, ΔH undergoes a more negative value of about -1300 nT at the day side around 04:00 UT and the ΔTEC attains a positive value of around 40% at Mawson station in the southern hemisphere.

This may be due to the interactions between IMF Bz and the magnetosphere, which in turn lead to energy, momentum transfer, and electric current movement in the ionosphere.

A geomagnetic storm occurs when a large amount of energy enters the ionosphere from the solar wind. These energy increase the flow of energy and momentum in to the magnetosphere and the rate of convection [6]. Due to the collisions in the inner magnetosphere equator-ward existing auroral arc suddenly brightens and expands east and west ward during sub-storm in turns rapid changes of TEC over the stations [39].

4. Conclusion

The effects of the August 26, 2018 geomagnetic storm on ionospheric TEC variability over two GPS sites in the northern and southern hemispheres provide an outstanding chance to examine ionospheric TEC variability.

1. The variability of TEC over Hofn and Kiruna stations in the northern hemisphere indicates that there was a greater value of TEC over Hofn station than over Kiruna during the initial phase on August 25, 2018 between 12:00 UT and 23:59 UT. But, TEC was enhanced more over Syog than Mawson station during the day side of the main phase of the storm. This may be due to the effect of solar heating conditions exercised over the stations, with the sun-side over one station and the clouded part over the other stations.
2. The positive enhancement of TEC was observed during the main phase of the storm, having values of about 170% and 180% over Hofn and Kiruna stations, respectively, at 05:00 UT. Similarly, at 05:00 UT of the main phase, changes in TEC value over Mawson and Syog stations were observed to be between 70% and 150%, indicating that changes in TEC over northern stations were enhanced more than changes in TEC over southern stations during the suggested geomagnetic storm.
3. At Mawson station, the enhancement of TEC shows opposite trends to those at other Syog, Hofn, and Kiruna stations during the initial and recovery phases of the storm. On August 25, 2018, the changes in TEC increased to 100%, and on August 27, 2018, the changes in TEC increased to 80% around 20:00 UT. This might be due to the effect of the thermosphere-ionosphere system on energy and momentum inputs from the solar wind plasma, interplanetary magnetic field (IMF), and the magnetosphere during the storm's initial phase, which involves nonlinear interactions of dynamical, chemical, and electrodynamical processes at various temporal and spatial scales [17].
4. Interestingly, during the main phase of the storm on August 26, 2018, the midnight TEC became comparable to the daytime TEC over both northern and southern sites, suggesting that the northern stations absorbed more plasma from higher latitudes than the southern stations.
5. Highly a negative impact on TEC is measured predominantly for Hofn and Kiruna about ΔTEC = -50% than Mawson and Syog stations ΔTEC=-40% during the August 26, 2018 geomagnetic storm respectively.
6. Plasma convection and auroral precipitation patterns expanded as magnetic activity increased, electric fields became stronger, convection speed increased, fast plasma flows occurred, and particle precipitation intensified at Kiruna and Hofn in the northern hemisphere and Syog and Mawson in the southern hemisphere. This may change the variability of TEC throughout all stations during the storm's main phase [40].
7. The variability of ΔTEC was more pronounced over the northern hemisphere of Hofn and Kiruna than in the southern hemisphere of Mawson and Syog stations. This may be due to the fact that, the two northern hemisphere stations are located around the Polar Regions, and when the storm happens TEC was extremely enhanced over the polar stations. Also, the northern hemisphere experiences summer during the month of August because it is tilted toward the sun and receives the most direct sunlight.
8. The changes in ionospheric TEC over each station are caused by a significant rise in the Kp index and the opposite polarity of the interplanetary electric field (IEF Ey) in the northward direction and the southward decrease of the interplanetary magnetic field (IMF Bz). The decrease in Dst-index and ΔH during the main phase of the storm increases changes in TEC (ΔTEC) over Kiruna and Mawson stations. Furthermore, the enhancement of changes in TEC was stronger over Kiruna station in the northern hemisphere than over Mawson station in the southern hemisphere, indicating that the northern stations received more additional plasma than the southern stations during the August 26, 2018 geomagnetic storm.
9. Finally, during the August 26, 2018 geomagnetic storm, decreasing values of ΔH were more pronounced over the northern hemisphere of Kiruna station about ΔH = -1500 nT than over the southern hemisphere of Mawson station about ΔH = -1300 nT due to the enhancements of ring currents and, when such a difference happens, the changes in TEC are more enhanced over the northern hemisphere (ΔTEC = 180% over Kiruna) than the southern hemisphere (ΔTEC = 70% over Mawson),

and this might be because the northern hemisphere receives more energy from the solar wind, which produces particle acceleration and precipitation, higher field aligned currents, and ionospheric electrojets [41].

In general, when the interplanetary magnetic field's Bz component is in the southward direction (negative), the ionospheric total electron content fluctuates more over all stations in the northern and southern hemispheres [42]. It is well understood that impulsive changes in solar wind parameters cause geomagnetic storms. When the component Bz is negative (southward), a reconnection or coupling with the geomagnetic field occurs, resulting in a large amount of energy deposition into the high latitude regions of the Earth [24].

Acknowledgements

My special thank goes to the datasets generated for this study can be found in the International GNSS Service (IGS), (http://www.unavco.org/data/gps-gnss/data/), and Omni website data sets from (https://omniweb.gsfc.nasa.gov/). Finally, the author wish to appreciate the Magnetic Observatory Network INTERMAGNET website http://www.intermagnet.org).

References

[1] F. D'ujanga, P. Baki, J. Olwendo, and B. Twinamasiko, "Total electron content of the ionosphere at two stations in east africa during the 24–25 october 2011 geomagnetic storm," *Advances in Space Research*, vol. 51, no. 5, pp. 712–721, 2013.

[2] E. A. Ariyibi, E. O. Joshua, and B. A. Rabiu, "Studies of ionospheric variations during geomagnetic activities at the low-latitude station, ile-ife, nigeria," *Acta Geophysica*, vol. 61, no. 1, pp. 223–239, 2013.

[3] R. S. Fayose, R. Babatunde, O. Oladosu, and K. Groves, "Variation of total electron content [tec] and their effect on gnss over akure, nigeria," *Applied Physics Research*, vol. 4, no. 2, p. 105, 2012.

[4] A. Jain, S. Tiwari, S. Jain, and A. Gwal, "Tec response during severe geomagnetic storms near the crest of equatorial ionization anomaly," *94.20. Vv; 94.30. Lr*, 2010.

[5] W. D. Gonzalez, B. T. Tsurutani, and A. L. Clúa de Gonzalez, "Interplanetary origin of geomagnetic storms," *Space Science Reviews*, vol. 88, no. 3, pp. 529–562, 1999.

[6] C. Russell, "The solar wind interaction with the earth's magnetosphere: A tutorial," *IEEE transactions on plasma science*, vol. 28, no. 6, pp. 1818–1830, 2000.

[7] W. H. Campbell, "Geomagnetic storms, the dst ring-current myth and lognormal distributions," *Journal of Atmospheric and Terrestrial Physics*, vol. 58, no. 10, pp. 1171–1187, 1996.

[8] B. T. Tsurutani, G. S. Lakhina, and R. Hajra, "The physics of space weather/solar-terrestrial physics (stp): what we know now and what the current and future challenges are," *Nonlinear Processes in Geophysics*, vol. 27, no. 1, pp. 75–119, 2020.

[9] L. J. Paxton, Y. Zhang, H. Kil, and R. K. Schaefer, "Exploring the upper atmosphere: Using optical remote sensing," *Upper Atmosphere Dynamics and Energetics*, pp. 487–522, 2021.

[10] C.-C. Wu and R. Lepping, "Effects of magnetic clouds on the occurrence of geomagnetic storms: The first 4 years of wind," *Journal of Geophysical Research: Space Physics*, vol. 107, no. A10, pp. SMP–19, 2002.

[11] S. Basu, S. Basu, C. Valladares, H.-C. Yeh, S.-Y. Su, E. MacKenzie, P. Sultan, J. Aarons, F. Rich, P. Doherty, *et al.*, "Ionospheric effects of major magnetic storms during the international space weather period of september and october 1999: Gps observations, vhf/uhf scintillations, and in situ density structures at middle and equatorial latitudes," *Journal of Geophysical Research: Space Physics*, vol. 106, no. A12, pp. 30389–30413, 2001.

[12] H. U. Frey, "Localized aurora beyond the auroral oval," *Reviews of Geophysics*, vol. 45, no. 1, 2007.

[13] A. Richmond and G. Lu, "Upper-atmospheric effects of magnetic storms: a brief tutorial," *Journal of Atmospheric and Solar-Terrestrial Physics*, vol. 62, no. 12, pp. 1115–1127, 2000.

[14] P. Khatarkar, P. Bhawre, V. Kachneria, P. Purohit, and A. Gwal, "Behavior of total electron content over auroral region at maitri, antarctica," *International Journal of Scientific & Engineering Research*, vol. 5, no. 9, pp. 1–7, 2014.

[15] M. Abdu, "Equatorial ionosphere–thermosphere system: Electrodynamics and irregularities," *Advances in Space Research*, vol. 35, no. 5, pp. 771–787, 2005.

[16] P. R. Fagundes, F. Cardoso, B. Fejer, K. Venkatesh, B. Ribeiro, and V. Pillat, "Positive and negative gps-tec ionospheric storm effects during the extreme space weather event of march 2015 over the brazilian sector," *Journal of Geophysical Research: Space Physics*, vol. 121, no. 6, pp. 5613–5625, 2016.

[17] W. Wang, J. Lei, A. G. Burns, S. C. Solomon, M. Wiltberger, J. Xu, Y. Zhang, L. Paxton, and A. Coster, "Ionospheric response to the initial phase of geomagnetic storms: Common features," *Journal of Geophysical Research: Space Physics*, vol. 115, no. A7, 2010.

[18] B. Tsurutani, A. Mannucci, B. Iijima, M. A. Abdu, J. H. A. Sobral, W. Gonzalez, F. Guarnieri, T. Tsuda, A. Saito, K. Yumoto, *et al.*, "Global dayside ionospheric uplift and enhancement associated with interplanetary electric fields," *Journal of Geophysical Research: Space Physics*, vol. 109, no. A8, 2004.

[19] S. Basu, E. MacKenzie, S. Basu, H. Carlson, D. Hardy, F. Rich, and R. Livingston, "Coordinated measurements of low-energy electron precipitation and scintillations/tec in the auroral oval," *Radio science*, vol. 18, no. 6, pp. 1151–1165, 1983.

[20] R. Dabas, P. Bhuyan, T. Tyagi, R. Bhardwaj, and J. Lal, "Day-to-day changes in ionospheric electron content at low latitudes," *Radio science*, vol. 19, no. 03, pp. 749–756, 1984.

[21] P. Doherty, E. Raffi, J. Klobuchar, and M. B. El-Arini, "Statistics of time rate of change of ionospheric range delay," in *Proceedings of ION GPS-94, part*, vol. 2, 1994.

[22] E. Astafyeva, Y. Yasyukevich, A. Yasyukevich, B. Maletckii, and S. Syrovatskii, "High-latitude ionospheric irregularities during the 25–26 august 2018 geomagnetic storm as seen by ground-based and space-borne instruments," in *2021 XXXIVth General Assembly and Scientific Symposium of the International Union of Radio Science (URSI GASS)*, pp. 1–4, IEEE, 2021.

[23] D. Blagoveshchensky and M. Sergeeva, "Ionospheric parameters in the european sector during the magnetic storm of august 25–26, 2018," *Advances in Space Research*, vol. 65, no. 1, pp. 11–18, 2020.

[24] G. A. Mansilla, "Behavior of the total electron content over the arctic and antarctic sectors during several intense geomagnetic storms," *Geodesy and Geodynamics*, vol. 10, no. 1, pp. 26–36, 2019.

[25] O. Bolaji, J. Fashae, S. Adebiyi, C. Owolabi, B. Adebesin, R. Kaka, J. Ibanga, M. Abass, O. Akinola, B. Adekoya, *et al.*, "Storm time effects on latitudinal distribution of ionospheric tec in the american and asian-australian sectors: August 25–26, 2018 geomagnetic storm," *Journal of Geophysical Research: Space Physics*, vol. 126, no. 8, p. e2020JA029068, 2021.

[26] A. Van Dierendonck, J. Klobuchar, and Q. Hua, "Ionospheric scintillation monitoring using commercial single frequency c/a code receivers," in *proceedings of ION GPS*, vol. 93, pp. 1333–1342, 1993.

[27] I. Cherniak and I. Zakharenkova, "Large-scale traveling ionospheric disturbances origin and propagation: Case study of the december 2015 geomagnetic storm," *Space Weather*, vol. 16, no. 9, pp. 1377–1395, 2018.

[28] I. Cherniak and I. Zakharenkova, "High-latitude ionospheric irregularities: differences between ground- and space-based gps measurements during the 2015 st. patrick's day storm," *Earth, Planets and Space*, vol. 68, no. 1, pp. 1–13, 2016.

[29] A. O. Olabode and E. A. Ariyibi, "Geomagnetic storm main phase effect on the equatorial ionosphere over ile–ife as measured from gps observations," *Scientific African*, vol. 9, p. e00472, 2020.

[30] C. S. Carrano and K. M. Groves, "The gps segment of the afrl-scinda global network and the challenges of real-time tec estimation in the equatorial ionosphere," in *Proceedings of the 2006 National Technical Meeting of The Institute of Navigation*, pp. 1036–1047, 2006.

[31] C. U. Idosa and K. S. Rikitu, "Effects of total solar eclipse on ionospheric total electron content over antarctica on 2021 December 4," *The Astrophysical Journal*, vol. 932, no. 1, p. 2, 2022.

[32] V. A. Eyelade, A. O. Adewale, A. O. akala, O. S. Bolaji, and A. B. Rabiu, "Studying the variability in the diurnal and seasonal variations in gps total electron content over nigeria," in *Annales Geophysicae*, vol. 35, pp. 701–710, Copernicus GmbH, 2017.

[33] J. Lean, R. Meier, J. Picone, and J. Emmert, "Ionospheric total electron content: Global and hemispheric climatology," *Journal of Geophysical Research: Space Physics*, vol. 116, no. A10, 2011.

[34] P. Bhuyan and R. R. Borah, "Tec derived from gps network in india and comparison with the iri," *Advances in Space Research*, vol. 39, no. 5, pp. 830–840, 2007.

[35] O. Verkhoglyadova, B. Tsurutani, A. Mannucci, M. Mlynczak, L. Hunt, L. Paxton, and A. Komjathy, "Solar wind driving of ionosphere-thermosphere responses in three storms near st. patrick's day in 2012, 2013, and 2015," *Journal of Geophysical Research: Space Physics*, vol. 121, no. 9, pp. 8900–8923, 2016.

[36] T. Yeeram, "Interplanetary drivers of daytime penetration electric field into equatorial ionosphere during cir-induced geomagnetic storms," *Journal of Atmospheric and Solar-Terrestrial Physics*, vol. 157, pp. 6–15, 2017.

[37] B. Adhikari, S. Dahal, and N. P. Chapagain, "Study of field-aligned current (fac), interplanetary electric field component (ey), interplanetary magnetic field component (bz), and northward (x) and eastward (y) components of geomagnetic field during supersubstorm," *Earth and Space Science*, vol. 4, no. 5, pp. 257–274, 2017.

[38] I. A. Daglis, R. M. Thorne, W. Baumjohann, and S. Orsini, "The terrestrial ring current: Origin, formation, and decay," *Reviews of Geophysics*, vol. 37, no. 4, pp. 407–438, 1999.

[39] L. Juusola *et al.*, "Observations of the solar wind-magnetosphere-ionosphere coupling," 2009.

[40] R. W. Schunk, P. M. Banks, and W. J. Raitt, "Effects of electric fields and other processes upon the nighttime high-latitude f layer," *Journal of Geophysical Research*, vol. 81, no. 19, pp. 3271–3282, 1976.

[41] B. Adhikari, B. Kaphle, N. Adhikari, S. Limbu, A. Sunar, R. K. Mishra, and S. Adhikari, "Analysis of cosmic ray, solar wind energies, components of earth's magnetic field, and ionospheric total electron content during solar superstorm of November 18–22, 2003," *SN Applied Sciences*, vol. 1, no. 5, pp. 1–10, 2019.

[42] I. Shagimuratov, A. Krankowski, I. Ephishov, Y. Cherniak, P. Wielgosz, and I. Zakharenkova, "High latitude tec fluctuations and irregularity oval during geomagnetic storms," *Earth, planets and space*, vol. 64, no. 6, pp. 521–529, 2012.

Biography

Chali Idosa Uga received the B.Sc. Degree in Physics from the University of Jimma in 2015 and the M.Sc. Degree in Space Physics from the University of Wollega in 2020. He is motivated to do research in the areas of solar physics, ionospheric physics, magnetohydrodynamics, and the effects of solar flares, coronal mass ejections, and geomagnetic storms over different regions of the ionosphere. He has served as a researcher and lecturer in physics at Jimma University, Ethiopia. Linked In profile: https://www.linkedin.com/in/chali-idosa-baa118233. Orchid: http://orcid.org/0000-0002-4699-8342